

# Low Barrier Nanomagnets as P-bits for Spin Logic

Rafatul Faria,<sup>1,\*</sup> Kerem Yunus Camsari,<sup>1</sup> and Supriyo Datta<sup>1,†</sup>

<sup>1</sup>*School of Electrical and Computer Engineering, Purdue University, IN, 47907*

(Dated: November 22, 2016)

It has recently been shown that a suitably interconnected network of tunable telegraphic noise generators or “p-bits” can be used to perform even precise arithmetic functions like a 32-bit adder. In this paper we use simulations based on the stochastic Landau-Lifshitz-Gilbert (sLLG) equation to demonstrate that similar impressive functions can be performed using unstable nanomagnets with energy barriers as low as a fraction of a kT. This is surprising since the magnetization of low barrier nanomagnets is not telegraphic with discrete values of  $\pm 1$ . Rather it fluctuates randomly among all values between  $-1$  and  $+1$ , and the output magnets are read with a thresholding device that translates all positive values to 1 and all negative values to zero. We present sLLG-based simulations demonstrating the operation of a 32-bit adder with a network of several hundred nanomagnets, exhibiting a remarkably precise correlation: The input magnets  $\{A\}$  and  $\{B\}$  as well as the output magnets  $\{S\}$  all fluctuate randomly and yet the quantity  $A+B-S$  is sharply peaked around zero! If we fix  $\{A\}$  and  $\{B\}$ , the sum magnets  $\{S\}$  rapidly converge to a unique state with  $S=A+B$  so that the system acts as an adder. But unlike standard adders, the operation is invertible. If we fix  $\{S\}$  and  $\{B\}$ , the remaining magnets  $\{A\}$  converge to the difference  $A=S-B$ . These examples suggest a new direction for the field of nanomagnetism away from stable high barrier magnets towards stochastic low barrier magnets which not only operate with lower currents, but are also more promising for continued downscaling.

## I. INTRODUCTION

The developments in spintronics and nanomagnetism are having enormous influence on the field of storage and memory devices and it has been shown that the WRITE (W) and READ (R) elements can also be integrated into units that implement Boolean as well as non-Boolean logic [1–8]. These applications, however, usually make use of stable magnets with energy barriers  $\sim 40$  kT which require relatively large currents for their operation. The critical spin current needed to switch a magnet with a thermal energy barrier of  $\Delta = H_K M_s V/2$  is given by [9]

$$I_c = I_{c0} \frac{\Delta}{kT} \quad (1a)$$

$$I_{c0} = \frac{4q\alpha}{\hbar} kT (1 + f_I \frac{H_d}{2H_K}) \quad (1b)$$

where  $q$  is the electronic charge,  $M_s$  is the saturation magnetization,  $H_K$  is the anisotropy field,  $H_d$  is the demagnetization field,  $V$  is the volume,  $\alpha$  is the Gilbert damping coefficient and the factor  $f_I$  is equal to zero for perpendicular anisotropy magnets (PMA) and one for in-plane anisotropy magnets (IMA). With  $\Delta \sim 40$  kT and  $\alpha \sim 0.01$ , the critical switching spin current for a PMA magnet is  $4q\alpha\Delta/\hbar \approx 10 \mu A$ . Magnets with lower barriers could operate with lower currents but their application in conventional memory or logic is severely limited due

to their stochastic nature. However, their possible use in unconventional applications has been discussed both theoretically and experimentally [10–18]. The implementation of logic operations based on an ensemble average over stable nanomagnets has been explored in [19–21] while [26] describes an approach to the traveling salesman problem based on a time average over unstable nanomagnets that cycle through millions of collective correlated states potentially at GHz rates. The present paper describes the application of the latter approach to implement precise Boolean logic operations like a 32-bit adder that provides the sum  $S$  for given inputs  $A$  and  $B$ . Remarkably the adder also evaluates the inverse function, cycling through all combinations of  $A$  and  $B$  that add up to a given sum  $S$ .

We have recently shown [22] that a suitably interconnected network of tunable telegraphic noise generators or “p-bits” can be used to perform even precise arithmetic functions like a 32-bit adder. However, it is not clear whether such p-bits can be implemented with real physical systems, especially if the noise in these systems are not telegraphic but continuous. The objective of this paper is to use simulations based on the stochastic Landau-Lifshitz-Gilbert (sLLG) equation to demonstrate that p-bits can be implemented using unstable nanomagnets with energy barriers as low as a fraction of a kT, *even though their magnetization is not telegraphic* and fluctuate randomly among all values from  $-1$  to  $+1$ . We assume that the magnets are read with a thresholding device that translates all positive values to 1 and all negative values to zero. But this thresholding is applied *only* when we need to read a magnet at the end of an operation.

**Outline of paper:** We start in *Section 2* by showing that low barrier magnets, both PMA and IMA, exhibit the key property of p-bits, namely that they act as

\* rfaria@purdue.edu

† datta@purdue.edu

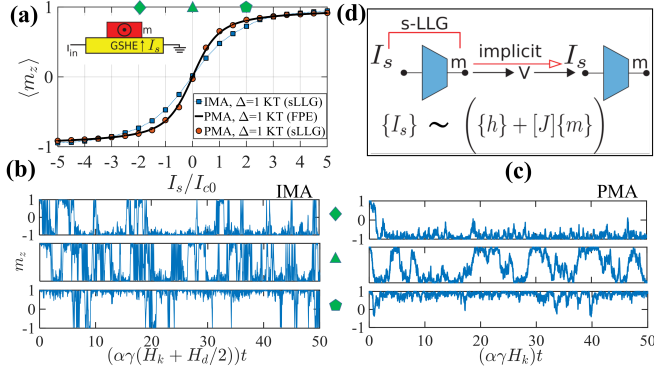


**FIG. 1. Low-barrier stochastic Nanomagnet as a p-bit:** (a) Time-averaged magnetization of low barrier IMA and PMA magnets ( $\Delta = 1$  kT,  $H_K = 60$  mT,  $\alpha = 0.01$ ,  $H_d = 1.5$  T for IMA) as a function of the bias spin current which is normalized to  $I_{c0}$  (Eq. 1b). Average magnetization of PMA magnets obtained from sLLG which agrees well with the analytical solution from the FPE, Eq. 7. Inset shows a physical structure using a giant spin Hall effect (GSHE) material that could be used to convert a charge current into a spin current with the correct polarization to bias an IMA. (b) The magnetization  $m(t)$  for IMA as a function of time for three different bias currents obtained from a numerical solution of sLLG equation. (c) Same plot for PMA with the same barrier height. Note that the fluctuations are much faster and more telegraphic for IMA than for PMA. (d) A connection scheme for two p-bits is shown where the magnetization of a p-bit is implicitly converted into the bias current/voltage for the next p-bit (Eq. 2).

electrically tunable random number generators (RNG). Their magnetization  $m(t)$  fluctuates randomly in time, and the time-averaged  $\langle m \rangle$  can be tuned from  $-1$  to  $+1$  with a spin current. It is well known that stable PMA magnets ( $f_I = 0$ , Eq. 1b) have a lower critical switching current compared to IMA ( $f_I = 1$ ). Interestingly for both PMA and IMA magnets, the current needed to tune the average magnetization from say  $-0.8$  to  $+0.8$  is approximately the corresponding current needed to switch a magnet with a 1 kT barrier. This means that IMA magnets require a larger current to tune, but this is offset by a more rapid fluctuation rate, allowing a faster evaluation of the time average, and hence faster operation (Fig. 1). Note also that the PMA magnetization is relatively continuous compared to IMA magnetization which is more telegraphic in nature.

Both PMA and IMA stochastic nanomagnets provide a random magnetization whose average depends on the input current. To harness them for logic applications, they have to be interconnected such that the spin current  $I_{sk}$  driving magnet 'k' has to be derived from the magnetization of other magnets.

$$\frac{2I_{sk}}{I_{c0}} = -I_0 \left( h_k + \sum_j J_{kj} m_j \right) \quad (2)$$

where  $I_{c0}$  is the critical current (Eq. 1b) for a magnet

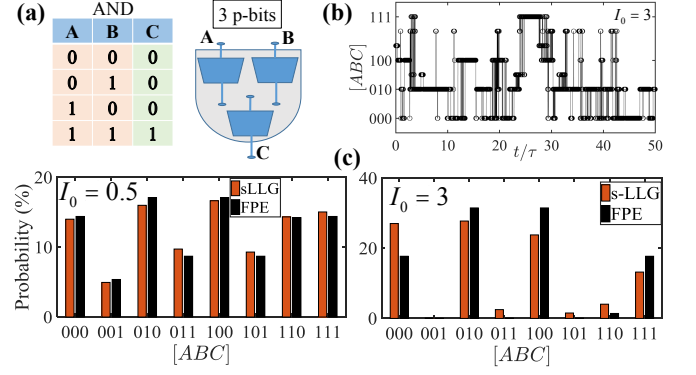


**FIG. 2. Implementation of a basic boolean element (AND) using p-bits:** (a) The truth table for AND is shown along with a schematic for the network of three p-bits used to perform the operation. The p-bits are connected symmetrically with  $J_{ij} = J_{ji}$ . (b) The decimal value of each configuration of the input-output nodes at each time step (normalized by the factor  $\tau = (\alpha\gamma(H_k + H_d/2))^{-1}$ ) is calculated according to  $A \times 2^2 + B \times 2^1 + C \times 2^0$  where A, B and C are thresholded to obtain binary values (0,1) at the read out. (c) Histograms of the different configurations of the p-bits are shown for a weaker ( $I_0 = 0.5$ ) and stronger ( $I_0 = 3$ ) correlation strength. Note the close match between the numerical values obtained from the sLLG equation with the probabilities obtained analytically from the FPE result in Eq. 8 which is related to the Boltzmann law, especially for  $I_0=0.5$ . For higher values of  $I_0$  the numerical results tend to be stuck in metastable states requiring longer simulation times to converge to the steady-state FPE result.

with a barrier  $\Delta = 1$  kT and  $I_0$  determines the overall strength of the interconnections. The bias  $\{h\}$  and interconnection  $[J]$  matrices have to be designed appropriately in implementing specific operations. We will not go into the implementation of these matrices since there are many options requiring careful discussion [3],[6],[23],[24]. We will assume that a network of stochastic nanomagnets (PMA and IMA) has been interconnected according to Eq. 2 and simulate their behavior using the stochastic Landau-Lifshitz-Gilbert (sLLG) equation to demonstrate useful functionalities. All numerical examples are presented for IMA but similar results are obtained with PMA as well.

In Section 3 we describe how simple logic gates can be implemented by suitably designing the  $\{h\}$  and  $[J]$  matrices so that the magnet configurations corresponding to the desired truth table represent 'low energy' states where the network spends most of its time according to the Boltzmann law of equilibrium probabilities

$$P(\{m\}) \sim \exp \left( - \frac{E(\{m\})}{kT} \right) \quad (3)$$

Although the use of spin currents does not in general permit us to write an energy functional [25], for symmetrically interconnected PMA magnets we can use a

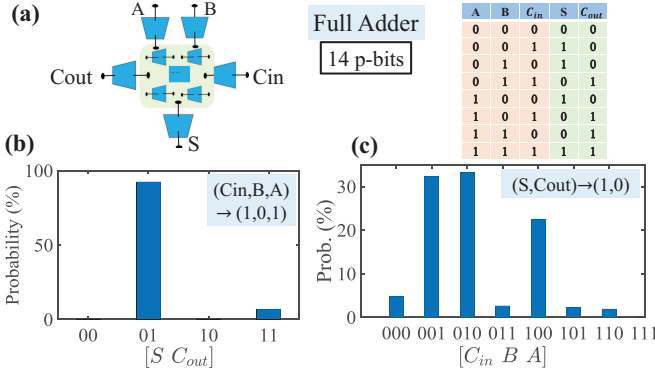


**FIG. 3. Full Adder:** (a) A full adder (truth table shown) implemented by connecting 14 p-bits symmetrically. (b) In forward mode, when the inputs ( $A, B, C_{in}$ ) are clamped, the adder gives the correct output ( $S$  and  $C_{out}$ ). (c) Unlike standard logic, these gates are *invertible*: If the output nodes of the adder are clamped to fixed values, the adder gives all possible input combinations satisfying the output constraint.

functional of the form [26]

$$-\frac{E(\{m\})}{kT} = \sum_i \frac{\Delta_i}{kT} m_i^2 + I_0 \left( \sum_i h_i m_i + \frac{1}{2} \sum_{i,j} J_{ij} m_i m_j \right) \quad (4)$$

to describe the network of interconnected magnets. This can be seen by noting that from Eqs. 3 and 4

$$\frac{\partial \ln P}{\partial m_k} = 2 \frac{\Delta_k}{kT} m_k + I_0 \left( h_k + \frac{1}{2} \sum_j (J_{kj} + J_{jk}) m_j \right)$$

so that for a symmetric  $[J]$  matrix, from Eq. 2

$$P(m_k) \sim \exp \left( \frac{\Delta_k}{kT} m_k^2 - \frac{2I_{sk}}{I_{c0}} m_k \right) \quad (5)$$

which is exactly the steady-state condition for magnet ‘k’ that we would obtain from the Fokker-Planck equation (FPE) ([27] Eq. (3.9)) for PMA. We will refer to Eqs. 3 and 4 as the FPE probability.

The probability distributions obtained from the numerical solution of the sLLG equation for both PMA and IMA magnets follow the FPE result quite well (Fig. 2). The highest probabilities correspond to the lowest energy states, which correspond to the desired truth table relating the input magnets A and B to the output magnet C. If we force the inputs A and B to specific values by using appropriate values for  $h_A$  and  $h_B$ , C would take on the specific value required by the truth table, just like standard digital gates. But unlike standard gates, these gates are invertible, similar to those discussed in the context of memcomputing [28]. They can be operated in reverse: if we clamp the output C to a specific value, the inputs

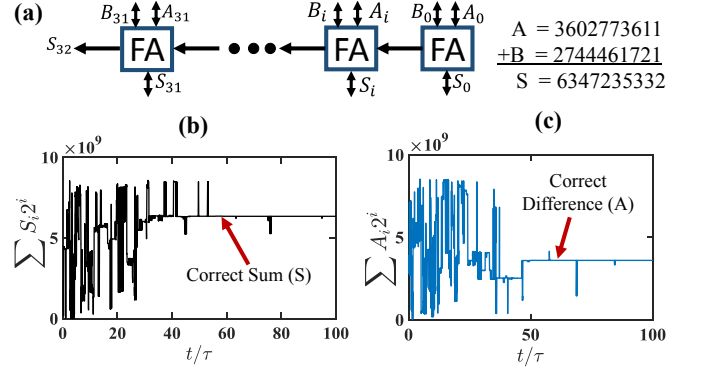


**FIG. 4. 32-bit Adder/ Subtractor:** (a) Schematic of an adder constructed from 32 full adders (from Fig. 3) with the carry out bit  $C_{out}$  from each adder communicated in a directed fashion to the carry in bit  $C_{in}$  of the next adder. (b) Time evolution of the sum  $S = \sum_i S_i 2^i$  obtained from the sum bits  $\{S\}$  as the coupling strength  $I_0$  is ramped up starting from zero. Note that in a time  $\sim 60 \tau$  ( $\tau$  is defined in Fig. 2), the sum converges (with occasional jumps) to the correct value which represents one out of  $2^{33} \sim 8$  billion possibilities. (c) Although the individual adders are connected in a directed fashion through the carry bits, the overall 32-bit adder performs the inverse function as well. If the sum bits  $\{S\}$  are clamped along with one set of input (B), the other input converges rapidly to the correct difference (A).

A and B will spend most of its time in those configurations  $\{AB\}$  that produce that output. We also illustrate this reversible operation with a more complex logic gate, namely a full adder treating it as a Boltzmann machine (BM) and using the same principle of energy minimization to design the  $\{h\}$  and  $[J]$  matrices.

Finally in Section 5 we demonstrate the operation of a 32-bit adder obtained from 32 full adders with the output carry from each bit connected to the carry in of the next higher bit through the appropriate element of the overall  $[J]$  matrix. Note that these are unidirectional connections so that the overall  $[J]$  matrix is not symmetric, though the  $[J]$  matrix for each full adder is symmetric. We show that this network of nearly five hundred nanomagnets exhibits a remarkably precise correlation that provides the exact sum  $S$  of any two given inputs, A and B (Fig.4). What is even more remarkable is that if we do not fix either the inputs or the outputs, the quantities A, B and S all fluctuate randomly and yet the quantity  $A+B-S$  is sharply peaked around zero, so that the network can be used to extract either A, B or S, if the other two are fixed, which is similar to the NP-complete “subset sum” problem (Fig.5) [29, 30].

## II. STOCHASTIC NANOMAGNET MODEL

Fig.1(b,c) shows the time response of the magnetization  $m_z$  along the easy axis calculated using the sLLG equation with  $\Delta t = 0.95 \text{ ps}$  for IMA and  $\Delta t = 11.8 \text{ ps}$

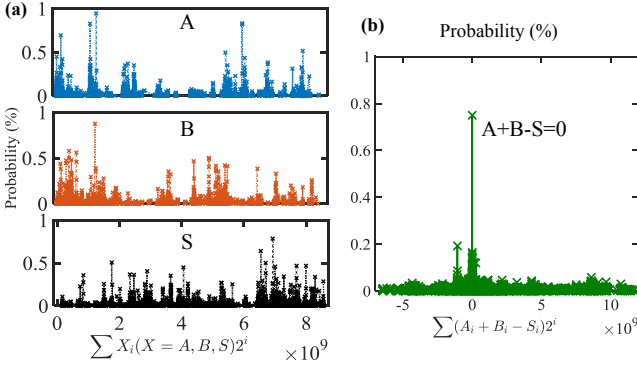


**FIG. 5. Correlated Adder:** A remarkable property of the adder (in Fig. 4) is that it works even when the inputs (A,B) and the output (S) are not unique and fluctuate in time amongst many allowed values as shown in (a). Nevertheless, the quantity  $A+B-S$  is sharply peaked at zero (b), demonstrating the correlation of hundreds of nanomagnets consistent with the addition function  $A+B-S=0$ .

for PMA.

$$(1 + \alpha^2) \frac{d\hat{m}_i}{dt} = -|\gamma| \hat{m}_i \times \vec{H}_i - \alpha |\gamma| (\hat{m}_i \times \hat{m}_i \times \vec{H}_i) + \frac{1}{qN_i} (\hat{m}_i \times \vec{I}_{Si} \times \hat{m}_i) + \left( \frac{\alpha}{qN_i} (\hat{m}_i \times \vec{I}_{Si}) \right) \quad (6a)$$

where  $H_i$  is the effective field including the uniaxial and shape anisotropy terms, as well as the thermally fluctuating magnetic field due to three dimensional uncorrelated thermal noise  $H_n$  having Gaussian distribution with mean  $\langle H_n \rangle = 0$  and standard deviation  $\langle H_n^2 \rangle = 2\alpha kT/|\gamma| M_s V$  along each direction [31–35],  $\gamma$  is the gyromagnetic ratio and  $N_i = M_s V/\mu_B$  is the total number of Bohr magnetons comprising the magnet. The time-averaged magnetization (Fig. 1a) obtained from the sLLG equation for PMA magnets is in good agreement with that obtained analytically by averaging over the FPE result (Eq. 5):

$$\langle m \rangle = \int_{-1}^{+1} dm \, m \, P(m) / \int_{-1}^{+1} dm \, P(m) \quad (7)$$

### III. BASIC BOOLEAN GATES

In implementing any given truth table we need the  $\{h\}$  and  $[J]$  matrices that make the truth table correspond to the lowest energy states of the energy functional given in Eq. 4. The choice of these matrices is not unique and [36] provides a suitable set for AND, OR gates along with many other functions. Fig. 2a shows one possible implementation of an AND gate using a network of three nanomagnets, representing A, B and C.

The magnetization of the magnets A, B and C fluctuates continuously between  $-1$  and  $+1$  and are mapped into the binary values of 0 and 1 by a thresholding oper-

ation: all negative values map to zero, while positive values map to  $+1$ . The y-axis in Fig. 2b shows the resulting binary number  $\{ABC\}$  converted into a single number  $A \times 2^2 + B \times 2^1 + C \times 2^0$ . Note how the values on the y-axis are clustered around 0, 2, 4 and 7 which correspond to the lines of the truth table shown in Fig. 2a. Occasionally the system jumps to other values but it quickly returns to one of these preferred values.

This clustering is reflected in the histogram constructed from 678 normalized time steps (Fig. 2c) which shows peaks around the preferred states defined by the truth table. This agrees well with the probability plot constructed from the FPE result in Eq. 3 noting that we can label the thresholded states with a binary variable  $s$ , where  $m_i = s_i m$  where  $s_i = \pm 1$  and  $0 < m < 1$  so that from Eq. 4

$$E(\{s\}, m) = \left( \sum_i \frac{\Delta_i}{kT} + \frac{1}{2} I_0 \sum_{i,j} J_{ij} s_i s_j \right) m^2 + \left( I_0 \sum_i h_i s_i \right) m$$

$$P(\{s\}) \sim \int_0^1 dm \exp(-E(\{s\}, m)) \quad (8)$$

Note that the probabilities are strongly affected by the choice of  $I_0$  as we might expect from the exponential dependence of the Boltzmann function. If we use a much smaller value of  $I_0$  we obtain a uniform probability across all eight states as we would expect for three uncorrelated magnets. If we use a much larger value of  $I_0$  the Boltzmann law predicts all states with equal energy to be equally occupied, but in a numerical simulation, the system tends to get stuck for long periods in one of the preferred states, instead of moving freely among them.

Consider now a full adder having three inputs  $A, B, C_{in}$  and two outputs  $S, C_{out}$ ,  $S$  being the sum bit, and  $C_{in}, C_{out}$  being the incoming carry and the outgoing carry bits. Fig. 3 shows a full adder constructed out of 14 p-bits treating it as a BM with a symmetric J-matrix which is obtained by a suitable extension of the principles developed in the context of Hopfield networks ([37], Eq. 4.20) and extended in [22]. This design not only gives the correct output for a given input, *but also the correct set of inputs for a given output*.

### IV. 32-BIT ADDER/SUBTRACTOR

Finally we demonstrate the operation of a 32-bit adder obtained from 32 full adders with a single directed connection from the  $C_{out}$  of one bit to the  $C_{in}$  of the next bit, in accordance with the standard design of ripple carry adders (RCA). If we provide two input numbers A and B, and look at the sum S, which includes all the sum bits along with the carry-out from the last bit,  $C_{out}(32)$  we find numerically that the histogram is sharply peaked around the correct sum. It is really quite surprising that a network of  $14 \times 32 = 448$  nanomagnets fluctuating continuously over the range  $-1 < m < +1$  get correlated

precisely enough to point to the correct answer out of  $2^{33} \approx 8$  *billion* possibilities. Interestingly it also works as a subtractor: if we fix the sum and one of the inputs B, the remaining input shows a clear peak at  $S-B$  (Fig. 4). Even more surprisingly, the overall system seems to act like a BM when all magnets are allowed to fluctuate. Each set of magnets A, B and S fluctuates randomly over a wide range of values. But the quantity  $A+B-S$  shows a sharp peak around zero (Fig. 5), showing that the interconnected network reflects the desired truth table.



## ACKNOWLEDGMENT

The authors gratefully acknowledge many helpful discussions with Behtash Behin-Aein (Globafoundries), Vinh Quang Diep (SanDisk), and with Ernesto E. Marinero (Purdue University). This work was supported in part by C-SPIN, one of six centers of STARnet, a Semi-

conductor Research Corporation program, sponsored by MARCO and DARPA, in part by the Nanoelectronics Research Initiative through the Institute for Nanoelectronics Discovery and Exploration (INDEX) Center, and in part by the National Science Foundation through the NCN-NEEDS program, contract 1227020-EEC.

- 
- [1] D. Bromberg, M. Moneck, V. Sokalski, J. Zhu, L. Pileggi, and J. Zhu, in *2014 International Electron Devices Meeting, San Francisco, CA, Session*, Vol. 33 (2014).
  - [2] S. Datta, S. Salahuddin, and B. Behin-Aein, *Applied Physics Letters* **101**, 252411 (2012).
  - [3] V. Q. Diep, B. Sutton, B. Behin-Aein, and S. Datta, *Applied Physics Letters* **104**, 222405 (2014).
  - [4] D. E. Nikonov and I. A. Young, *IEEE Journal on Exploratory Solid-State Computational Devices and Circuits* **1**, 3 (2015).
  - [5] S. Manipatruni, D. E. Nikonov, and I. A. Young, arXiv preprint arXiv:1512.05428 (2015).
  - [6] A. Sengupta, Y. Shim, and K. Roy, *IEEE Transactions on Biomedical Circuits and Systems* (2016).
  - [7] C. Pan and A. Naeemi, *IEEE Transactions on Nanotechnology* **15**, 820 (2016).
  - [8] M. G. Mankalale, Z. Liang, and S. S. Sapatnekar, arXiv preprint arXiv:1609.05141 (2016).
  - [9] J. Z. Sun, *Physical Review B* **62**, 570 (2000).
  - [10] N. Locatelli, A. Mizrahi, A. Accioly, R. Matsumoto, A. Fukushima, H. Kubota, S. Yuasa, V. Cros, L. G. Pereira, D. Querlioz, *et al.*, *Physical Review Applied* **2**, 034009 (2014).
  - [11] M. Bapna, S. K. Piotrowski, S. D. Oberdick, M. Li, C.-L. Chien, and S. A. Majetich, *Applied Physics Letters* **108**, 022406 (2016).
  - [12] S. K. Piotrowski, M. F. Matty, and S. A. Majetich, *IEEE Transactions on Magnetics* **50**, 1 (2014).
  - [13] W. H. Choi, Y. Lv, J. Kim, A. Deshpande, G. Kang, J.-p. Wang, and C. H. Kim, in *Electron Devices Meeting (IEDM)* (2014) pp. 12–5.
  - [14] A. Mizrahi, N. Locatelli, R. Lebrun, V. Cros, A. Fukushima, H. Kubota, S. Yuasa, D. Querlioz, and J. Grollier, *Scientific Reports* **6** (2016).
  - [15] G. Srinivasan, A. Sengupta, and K. Roy, *Scientific Reports* **6** (2016).
  - [16] A. F. Vincent, J. Larroque, N. Locatelli, N. B. Romdhane, O. Bichler, C. Gamrat, W. S. Zhao, J.-O. Klein, S. Galdin-Retailleau, and D. Querlioz, *IEEE transactions on biomedical circuits and systems* **9**, 166 (2015).
  - [17] S. Khasanvis, M. Li, M. Rahman, M. Salehi-Fashami, A. K. Biswas, J. Atulasimha, S. Bandyopadhyay, and C. A. Moritz, *IEEE Transactions on Nanotechnology* **14**, 980 (2015).
  - [18] N. Locatelli, A. F. Vincent, A. Mizrahi, J. S. Friedman, D. Vodenicarevic, J.-V. Kim, J.-O. Klein, W. Zhao, J. Grollier, and D. Querlioz, in *Proceedings of the 2015 Design, Automation & Test in Europe Conference & Exhibition (EDA Consortium, 2015)* pp. 994–999.
  - [19] B. Behin-Aein, V. Diep, and S. Datta, *Scientific Reports* **6**, 29893 (2016).
  - [20] Y. Bai and M. Lin, in *Proceedings of the 2016 ACM/SIGDA International Symposium on Field-Programmable Gate Arrays* (ACM, 2016) pp. 279–279.
  - [21] Y. Shim, A. Jaiswal, and K. Roy, arXiv preprint arXiv:1609.05926 (2016).
  - [22] K. Y. Camsari, R. Faria, B. M. Sutton, and S. Datta, arXiv preprint arXiv:1610.00377 (2016).
  - [23] J. J. Yang, D. B. Strukov, and D. R. Stewart, *Nature nanotechnology* **8**, 13 (2013).
  - [24] M. Yamaoka, C. Yoshimura, M. Hayashi, T. Okuyama, H. Aoki, and H. Mizuno, *Hitachi Review* **65**, 157 (2016).
  - [25] G. Bertotti, C. Serpico, I. D. Mayergoyz, A. Magni, M. d’Aquino, and R. Bonin, *Phys. Rev. Lett.* **94**, 127206 (2005).
  - [26] B. Sutton, K. Y. Camsari, B. Behin-Aein, and S. Datta, arXiv preprint arXiv:1608.00679 (2016).
  - [27] W. H. Butler, T. Mewes, C. K. Mewes, P. Visscher, W. H. Rippard, S. E. Russek, and R. Heindl, *IEEE Transactions on Magnetics* **48**, 4684 (2012).
  - [28] M. Di Ventra, F. L. Traversa, and I. V. Ovchinnikov, arXiv preprint arXiv:1609.03230 (2016).
  - [29] K. G. Murty and S. N. Kabadi, *Mathematical programming* **39**, 117 (1987).
  - [30] F. L. Traversa and M. Di Ventra, arXiv preprint arXiv:1512.05064 (2015).
  - [31] W. Scholz, T. Schrefl, and J. Fidler, *Journal of Magnetism and Magnetic Materials* **233**, 296 (2001).
  - [32] J. Z. Sun, *IBM journal of research and development* **50**, 81 (2006).
  - [33] B. Behin-Aein, D. Datta, S. Salahuddin, and S. Datta, *Nature nanotechnology* **5**, 266 (2010).
  - [34] W. F. Brown Jr, *Journal of Applied Physics* **34**, 1319 (1963).
  - [35] V. Q. Diep, “*Transistor-like spin nano-switches: Physics and applications*,” Ph.D. thesis, Purdue University (2015).
  - [36] J. Biamonte, *Physical Review A* **77**, 052331 (2008).
  - [37] D. J. Amit, *Modeling brain function: The world of attractor neural networks* (Cambridge University Press, 1992).